

Computational study on new natural polycyclic compounds of H1N1 influenza virus neuraminidase

Ye Wang · Di Wu · Dahai Yu · Zhiyong Wang · Li Tian · Yanyan Wang · Weiwei Han · Xuexun Fang

Received: 5 November 2011 / Accepted: 28 December 2011 / Published online: 27 January 2012
© Springer-Verlag 2012

Abstract A new strain of influenza A (H1N1) virus is a major cause of morbidity and mortality around the world. The neuraminidase of the influenza virus has been the most potential target for the anti-influenza drugs such as oseltamivir and zanamivir. However, the emergence of drug-resistant variants of these drugs makes a pressing need for the development of new neuraminidase inhibitors for controlling illness and transmission. Here a 3D structure model of H1N1 avian influenza virus neuraminidase type 1 (N1) was constructed based on the structure of the template H5N1 avian influenza virus N1. Upon application of virtual screening technique for N1 inhibitors, two novel compounds (ZINC database ID: ZINC02128091, ZINC02098378) were found as the most favorable interaction energy with N1. Docking results showed that the compounds bound not only in the active pocket, but also in a new hydrophobic cave which contains Arg368, Trp399, Ile427, Pro431 and Lys432 of N1. Our result suggested that both of the screened compounds containing the hydrophobic group bring a strong conjugation effect with Arg293, Arg368 Lys432 of N1 by pi-pi interaction. However, the control inhibitors zanamivir and oseltamivir do not have this effect. The details of N1-compound binding structure obtained will be valuable for the development of a new anti-influenza virus agent.

Keywords A H1N1 influenza virus · Homology modeling · Molecular docking · Neuraminidase · Virtual screening

Y. Wang · D. Wu · D. Yu · Z. Wang · L. Tian · Y. Wang · W. Han (✉) · X. Fang (✉)

Key Laboratory for Molecular Enzymology and Engineering of Ministry of Education, Jilin University, 2699 Qianjin Street, Changchun 130012, China
e-mail: weiwei.han@jlu.edu.cn
e-mail: fangxx@jlu.edu.cn

Introduction

A new strain of influenza A H1N1 virus, which shares several common characteristics with the 1918 Spanish flu, has spread rapidly and evolved into epidemics worldwide with high mortality and morbidity [1, 2]. Influenza virus can be classified by the antigenic properties of two surface glycoproteins, hemagglutinin (HA) and neuraminidase (NA) [3]. Hemagglutinin is known to mediate the binding of virus to the cell surface via sialic acid receptor which results in the cell entry of the virus [4–6]. Neuraminidase cleaves sialic acid receptor from cell surface, facilitating progeny virions' release from the infected host cells. Neuraminidase may also facilitate the early processing of influenza virus infection in lung epithelial cells [7]. Therefore, the inhibitions of influenza virus neuraminidase potentially block an influenza virus infection. Because of its importance in the pathogenesis of influenza virus infection, neuraminidase has been the most potential target for the anti-influenza drugs [8]. Two antiviral drugs, oseltamivir and zanamivir, both targeting neuraminidases, are currently prescribed for the prophylaxis and treatment of influenza infections.

However, although these drugs are effective against neuraminidase, the emergence of drug-resistant variants is the major problem of antiviral therapy [9]. Oseltamivir treatment showed resistance in up to 2% of patients in clinical trials and 18% of treated children including frequent resistance acquisition in the case of children only [10, 11]. Moreover, zanamivir-resistant influenza virus variants have been isolated from immuno-compromised patients [12].

In recent years, natural compound medicines have been increasingly reported showing anti-influenza virus activities [13, 14]. Natural compounds have been the mainstay of traditional medicine for thousands of years. The advantage of natural compounds for the development of drugs derives from their innate affinity for biological receptors and numerous

fractionated natural compounds have been screened with impressive hit rates [15]. Therefore, they may provide a valuable source of lead compounds for anti-influenza activities by inhibiting N1.

Recently, computer-based modeling methodology has been increasingly used to understand the mechanism of substrate inhibition and new drug development. It greatly improves test efficiency and reduces the experimental expenditure. In this study, homology modeling, virtual screening and molecular docking approach was used to find effective inhibitor of N1 and the mechanism of interaction between antiviral drugs and N1.

Methods

Sequence alignment and homology modeling

The amino acid sequence of H1N1 avian influenza virus N1 was collected from human Influenza A virus (A/reassortant/NYMC X-179A (California/07/2009 × NYMC X-157) (H1N1)) in the NCBI protein database (accession no. ACR47015.1), in which 469 amino acid residues were involved. Three structures were identified as homologous from Protein Data Bank (PDB) (PDB ID: 2C4A, 3CL0, 3CKZ). The automated sequence alignment (Fig. 1) and analysis of the template and target were carried out using the BioEdit Sequence Alignment Editor program [16]. The protein sequence chosen as template protein for homology

modeling was H5N1 avian influenza virus N1 (PDB ID: 3CKZ) [17], whose similarity equals 91.4% with the H1N1 avian influenza virus N1. Here, we used Swiss-Model [18–21] to build the 3D structure of H1N1 avian influenza virus N1 from their amino acid sequences. The model coordinates were returned in PDB format [22], and the structure was checked using Profile-3D [23] and PROCHECK [24].

Virtual screening

The software AutoDock Vina [25] which used a sophisticated gradient optimization method in its local optimization procedure was then applied in the virtual screening, with a rectangular box for the definition of the binding site. After setting the spacing (angstrom) to 1, the center and the size of the box could be defined and adjusted by AutoDock Tools software [26]. Here, parameter values of x, y, z center were set to -39.12, -73.82, and 40.91 to make grid center consistent with center of the protein. The parameter values of number of points in x,y,z-dimension were set to 44,44,40, so that the lattice could cover all of the protein atomic. A Natural Products Database (NPD) [27] in the ZINC [28, 29] database, which is the largest freely available database for docking and virtual screening methods, was employed to screen N1 inhibitors. The target used in our study was the 3D structure of N1 mentioned above. Modification and format conversion of compounds were downloaded from NPD using Open Babel toolbox [30] and Raccoon [31]

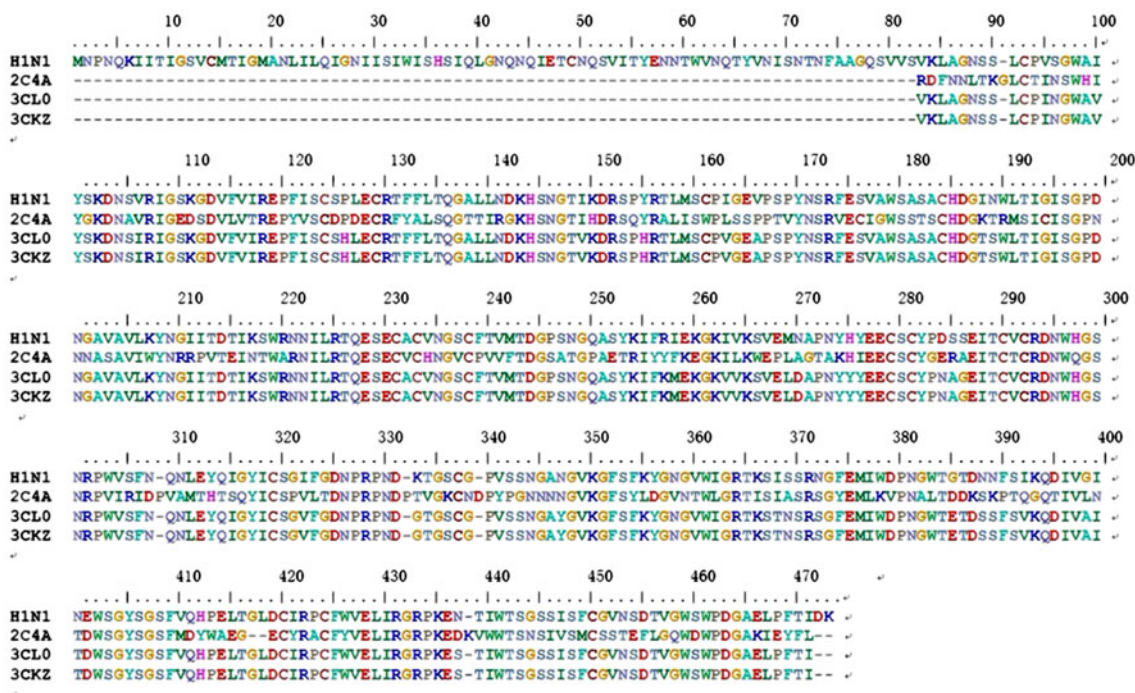


Fig. 1 N1 protein sequence aligned with three different template sequences

graphical user interface for AutoDock [26, 32] with a special focus on large-scale virtual screening.

Docking

The molecular docking was carried out with Affinity [33] program of the Insight II [34] software. Affinity is a suite of programs for automatically docking a ligand to a receptor, uses a combination of Monte Carlo type and simulated annealing (SA) methods. The 3D structures of the natural compounds were downloaded from NDP. After determining the active pocket by binding site Analysis program of the Insight II, the inhibitor was docked into N1. The potential function of the complexes was assigned by using the consistent-valence force field (CVFF) and non-bonding interaction was determined by using the cell multipole approach. To account for the solvent effect, the assemblies were solvated in a sphere of TIP3P water molecules with radius 15 Å around the binding site of inhibitor and the N1 complex. Finally, the docked complex was selected by the criteria of interacting energy combined with the geometrical matching quality. The obtained complex was used as the starting conformation for further energetic minimization before the final model was achieved. This provided 10 structures from SA docking and their generated conformations were clustered according to RMS deviation. The global structure with the most favorable interaction energy was chosen for computing intermolecular binding energies.

Results and discussion

Homology modeling of N1

The Swiss-Model program [18–21] was used to model the 3D structure of N1. As described above, the template (PDB ID: 3CKZ) we chose had too high homology to model the structure of N1, whose similarity equals 91.4%. Sequence alignment and structure superposition reveal that the active site of N1 is almost identical to that of the template, except for H274Y. This mutation abolished the hydrogen bond between the carboxyl group inhibitor and the template. However, the carboxyl group of the inhibitor formed a stronger hydrogen bond with Arg293 of N1 [35]. Thus, the binding affinity of the inhibitor with N1 was not reduced in comparison with that with the template, and retained the drug-sensitive from N1. Similar to the crystal structure of the template sequence, the structure of the model had two helices, 26 sheets, and 17 turns. By superimposing the 3D structure of template on the structure of the model, their root mean square deviation (RMSD) value was 0.07 Å (Fig. 2), which indicated a good overall structural alignment with template structure. The overall quality of the model was

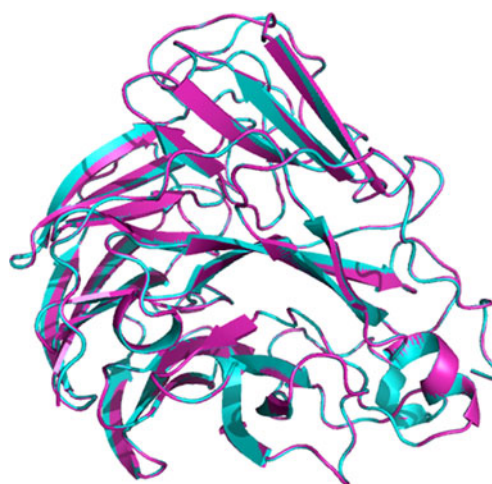


Fig. 2 Comparison of N1 model with its template protein H5N1 avian influenza neuraminidase (PDB ID: 2htyF). Magenta ribbon representation of N1. Cyan ribbon representation of H5N1 avian influenza neuraminidase. Their root mean square deviation (RMSD) value was 0.07 Å

examined by PROFILE-3D [23], and the self-compatibility score for this protein was 194.30, which was higher than the low score 78.99 and the top score 175.54. Figure 3 shows that the scores of all residues are positive value and correspond to ‘acceptable’ side chain environments. Then, the structure of the model was evaluated by PROCHECK [24], the statistical score of Ramachandran plot showed that 72.3% residues were in the most favored regions. By checking with the two different criteria mentioned above, we believed that the homology model of N1 was reliable.

Virtual screening of natural products database against N1

Virtual screening of compound libraries has become a standard technology in modern drug discovery pipelines [36]. A

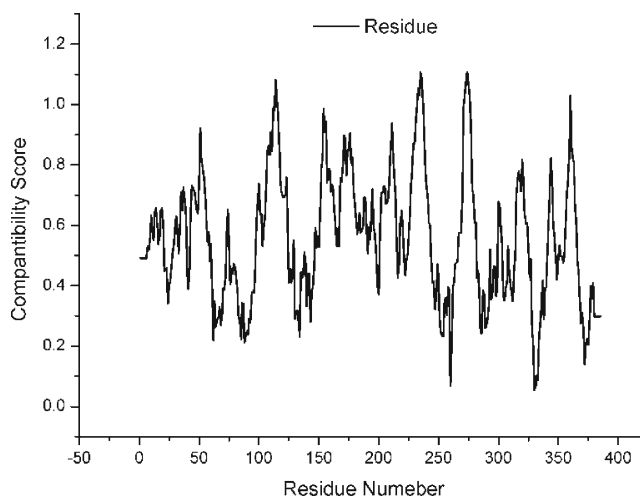


Fig. 3 The 3D profiles verified results of N1 model, residues with positive compatibility score are reasonably folded

good reliable library of natural compounds is required for virtual screening experimentally. NPD [27] contains compounds from seven vendors that advertise their compounds as being of natural origin, either pure natural products, or chemical derivatives of natural products. The "2008/5" version of the NPD contains almost 90,000 commercially available compounds. The target used in our study was the 3D structure of N1 mentioned above. In order to screen these compounds efficiently within a reasonable time, we used AutoDock Vina (a new open-source program for drug discovery) as that offering multi-core capability, high performance and enhanced accuracy and ease of use [25]. Affinity energy, which is the final calculated result and the core parameters of AutoDock Vina, is an important indicator of virtual screening of effective compounds. When calculating the affinity energy, spatial effects, rejection effect, hydrogen bonding, hydrophobic interactions, and molecular flexibility are taking into account.

After the screening, a large number of novel compounds were found as the favorable affinity energy with N1. Table 1 showed 34 of these compounds with lower $-11 \text{ kcal mol}^{-1}$ affinity energy. Two new natural compounds (ZINC database code ZINC02128091, ZINC02098378 Fig. 4a, b) with the most favorable interaction energy among these compounds were selected for further study.

Ligand binding analysis

In the molecular complex binding process, both the complementarily receptor-ligand binding site and the steric of ligand in the complex are the key factors. The electrostatic, Van der Waals, hydrogen bonding, hydrophobic interactions are the driving force behind the formation of molecular complex. In order to study ligand binding mechanism, the two compounds screened were docked into the 3D structure of N1 by using the Insight II/Affinity module. The total interaction energy as an estimation of molecular complex binding was used in this study. In the compound-neuraminidase complexes, both compounds bind to N1 in similar orientation (Fig. 5a-b) and some critical residues of N1 were identified, which suggested that the compounds had different binding modes compared to the positive anti-influenza drugs, zanamivir and oseltamivir as described below.

Both the novel compounds and the control drugs bound in the active pocket of N1 with strong total interaction energy and formed hydrogen bond interaction with N1

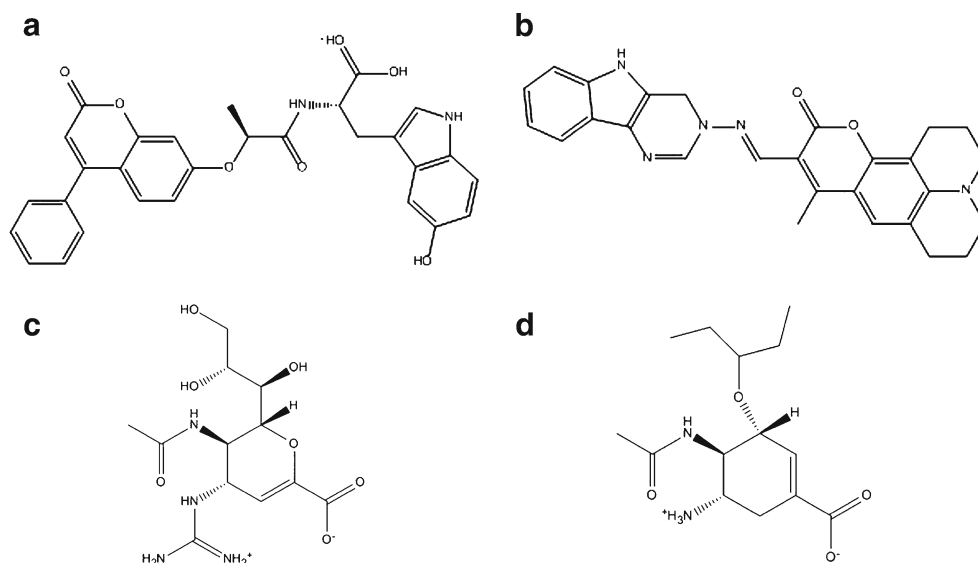
It had been reported in the literature that Arg118, Asp151, Glu278, Arg293, Asn344, Arg368, Tyr402 of N1 were in the active pocket [37, 38] which could form hydrogen bonds with its inhibitors. Our docking results in Fig. 5 showed that

Table 1 34 of these compounds from NPD with N1 have affinity energy lower $-11 \text{ (kcal mol}^{-1}\text{)}$

Compounds	Affinity (kcal mol ⁻¹)
ZINC02128091	-11.70
ZINC02098378	-11.70
ZINC02127309	-11.60
ZINC02097182	-11.50
ZINC02090662	-11.30
ZINC04015296	-11.30
ZINC04265785	-11.30
ZINC05433944	-11.30
ZINC02100657	-11.20
ZINC02103725	-11.20
ZINC04270571	-11.20
ZINC08877110	-11.20
ZINC08918445	-11.20
ZINC02103379	-11.10
ZINC02128147	-11.10
ZINC02129180	-11.10
ZINC04236083	-11.10
ZINC04259225	-11.10
ZINC04270586	-11.10
ZINC12296716	-11.10
ZINC12892580	-11.10
ZINC02105418	-11.00
ZINC02108251	-11.00
ZINC02118912	-11.00
ZINC02127034	-11.00
ZINC02150195	-11.00
ZINC03844856	-11.00
ZINC05433942	-11.00
ZINC08792177	-11.00
ZINC08877567	-11.00
ZINC08918259	-11.00
ZINC12858859	-11.00
ZINC12863203	-11.00
ZINC12874367	-11.00

ZINC02128091, ZINC02098378, zanamivir and oseltamivir, were tightly bound with the active site of N1. To identify the binding forces contributed to the N1-compound complexes, the Van der Waals energy (E_{Vdw}), electrostatic energy (E_{Eic}) and total interaction energy (E_{Inter}) of ZINC02128091, ZINC02098378, zanamivir and oseltamivir with N1 were calculated. The total interaction of receptor-ligand is the molecular recognition process, including electrostatic interaction, van der waals force, hydrogen bonding and hydrophobic interactions, etc. The values of the total interaction energy for oseltamivir and zanamivir shown in Table 2 were consistent with the experimental value [39–41]. Although the experimental data from different laboratories were different, most of them had similar trends that the inhibition constant

Fig. 4 The structures of two novel compounds from virtual screening. **(a)** ZINC02128091, **(b)** ZINC02098378. And the structures of anti-influenza drugs **(c)** zanamivir, **(d)** oseltamivir



of zanamivir was lower than oseltamivir, which was in good agreement with our calculated results. So, we account the order that ZINC02128091, ZINC02098378 ($-107.921 \text{ kcal mol}^{-1}$, $-89.2049 \text{ kcal mol}^{-1}$) had lower total interaction energy than the control drug zanamivir and oseltamivir ($-74.9895 \text{ kcal mol}^{-1}$, $-73.7462 \text{ kcal mol}^{-1}$). Moreover, the total interaction energy of ZINC02128091 was the most favorable.

Hydrogen bonds formed between compound and the active pocket of protein were usually contributed to the stability of the substrate-enzyme complexes, and more

hydrogen bonds form a more stable complex [42, 43]. In the present study, the N1-compound complex models were visualized by PYMOL molecular graphics system. As for the electron acceptor of the compounds, carbonyl O, carboxyl O, enol O and oxenium ion, were necessary to form hydrogen bonds with the catalytic active pocket of the protein. Our results shown that both the novel compounds formed a large number of hydrogen bonds as zanamivir and oseltamivir: N1-ZINC02128091 complex had four hydrogen bonds (Fig. 6), N1-ZINC02098378 complex had one hydrogen bonds (Fig. 7), zanamivir and oseltamivir, both

Fig. 5 Schematic drawing of interrelation between inhibitors and N1 by protein contact potential of vacuum electrostatics. Blue represents positive charge, red represents negative charge. Inhibitors are **(a)** ZINC02128091, **(b)** ZINC02098378, **(c)** zanamivir, **(d)** oseltamivir. All of inhibitors are located in the center of the active site of N1, tightly

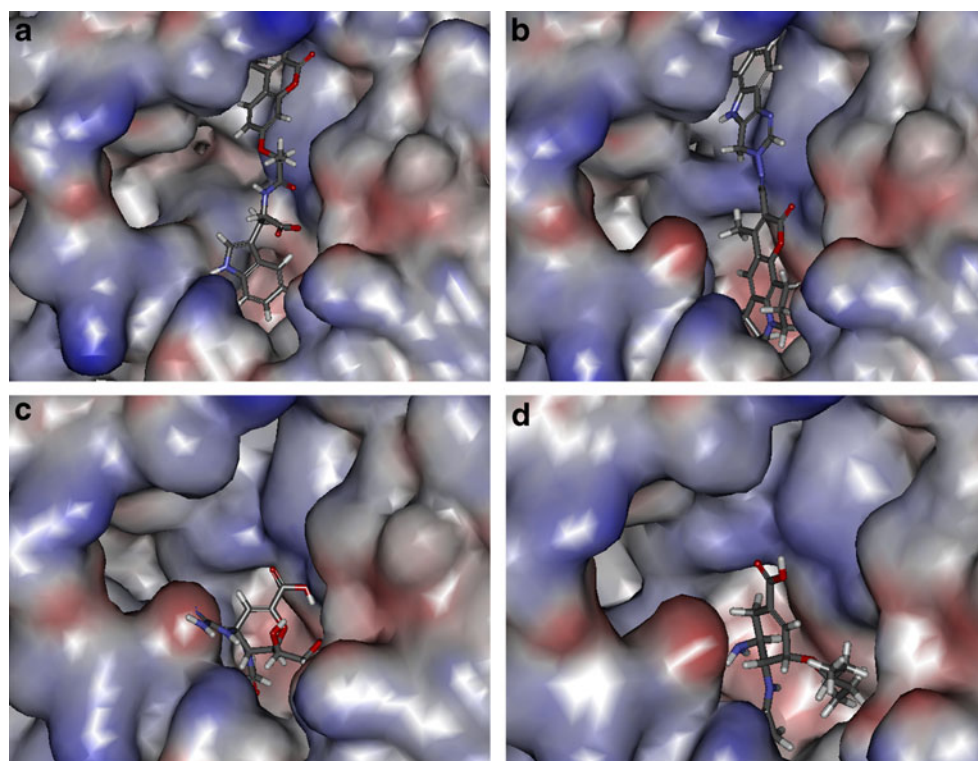


Table 2 The Van der Waals energy (E_{Vdw}), electrostatic energy (E_{Ele}), and total interaction energy (E_{Inter}) of ZINC02128091, ZINC02098378, zanamivir and oseltamivir with N1 (kcal mol⁻¹)

Compound	E_{Vdw}	E_{Ele}	E_{Inter}
ZINC02128091	-81.1144	-33.6364	-107.921
ZINC02098378	-78.9251	-28.0894	-89.2049
Zanamivir	-82.4703	-32.9628	-74.9895
Oseltamivir	-88.4223	-32.9152	-73.7462

formed four hydrogen bonds with N1, respectively (Figs. 8 and 9). It is worthy to note that ZINC02098378, which does not have as many electrophilic groups as the other three compounds, forms fewer hydrogen bonds with N1.

From analyzing the hydrogen bonds interaction, some critical N1 residues were identified (Table 3). The all focus the active pocket of N1, the residues of Arg118, Glu119, Asp151, Arg152, Arg156, Arg293 and Arg368 of N1 were considered to be important in the interaction. By means of analyzing the total interaction energy and the hydrogen bonds interaction, we consider that the novel compounds have a strong binding energy with N1 as the control drugs.

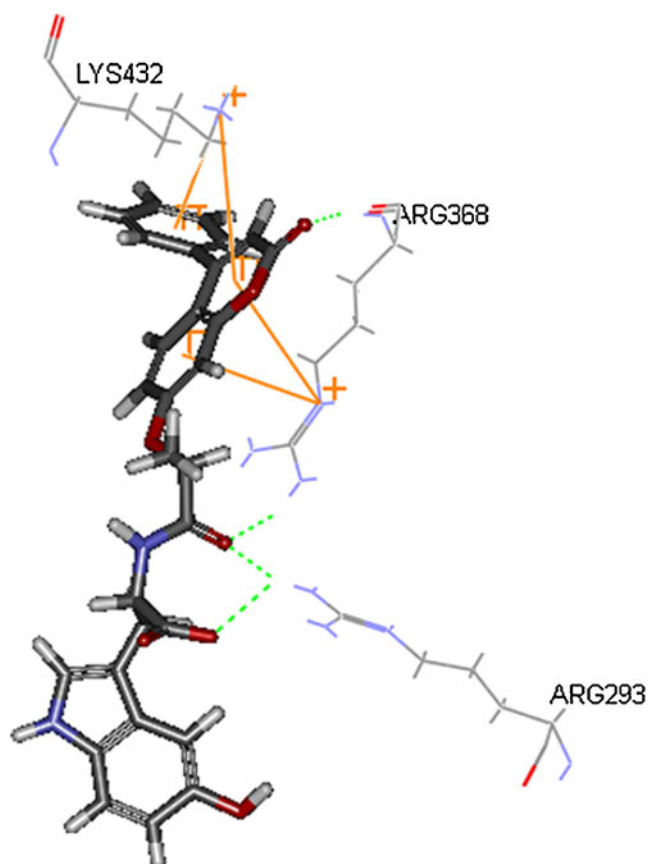


Fig. 6 Hydrogen bonds and pi-pi interaction formed between ZINC02128091 and the active site of N1. Hydrogen bonds are shown by green dash line. Pi-pi interactions are shown by yellow solid line

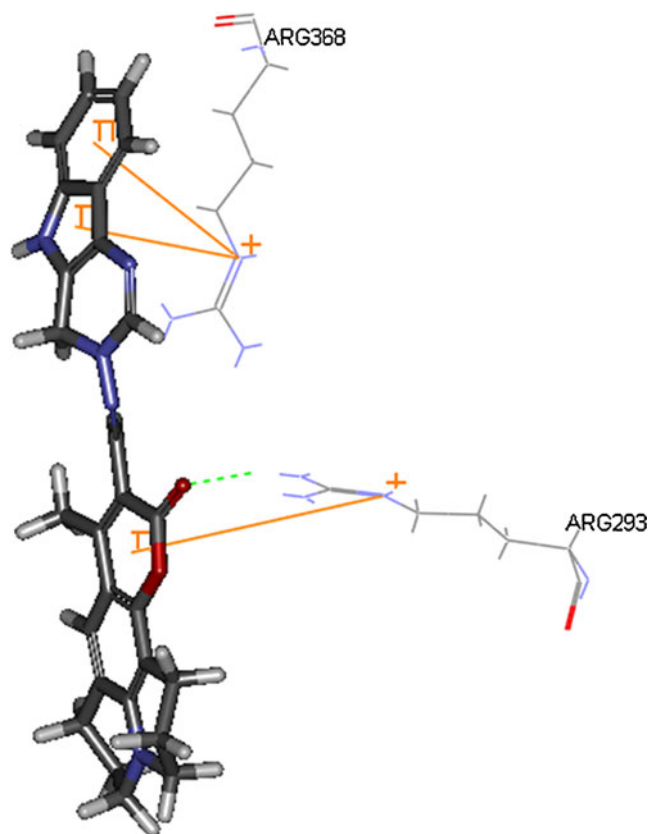


Fig. 7 Hydrogen bonds and pi-pi interaction formed between ZINC02098378 and the active site of N1. Hydrogen bonds are shown by green dash line. Pi-pi interactions are shown by yellow solid line

The novel compounds formed pi-pi interaction with N1

It could also be seen from Fig. 10 that both ZINC02128091 and ZINC02098378 bound not only in the active pocket, but also in a new hydrophobic cave which contains Arg368, Trp399, Ile427, Pro431 and Lys432 of N1, which brings a strong conjugation effect. Normal conjugated effect, also known as pi-pi interaction, is due to the formation of conjugated Pi bond caused by the effect of the molecular nature of the change [44]. By analyzing the pi-pi interaction results (Table 4), Arg368 and Lys432 of hydrophobic cave in N1

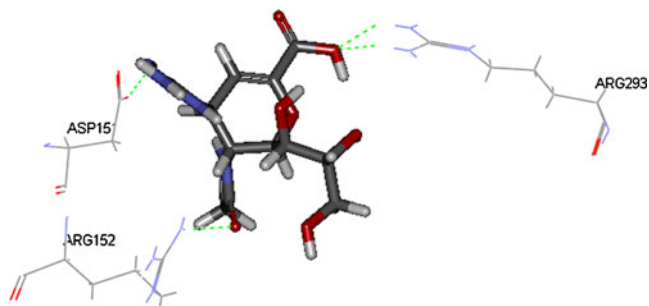


Fig. 8 Hydrogen bonds formed between zanamivir and the active site of N1. Hydrogen bonds are shown by green dash line

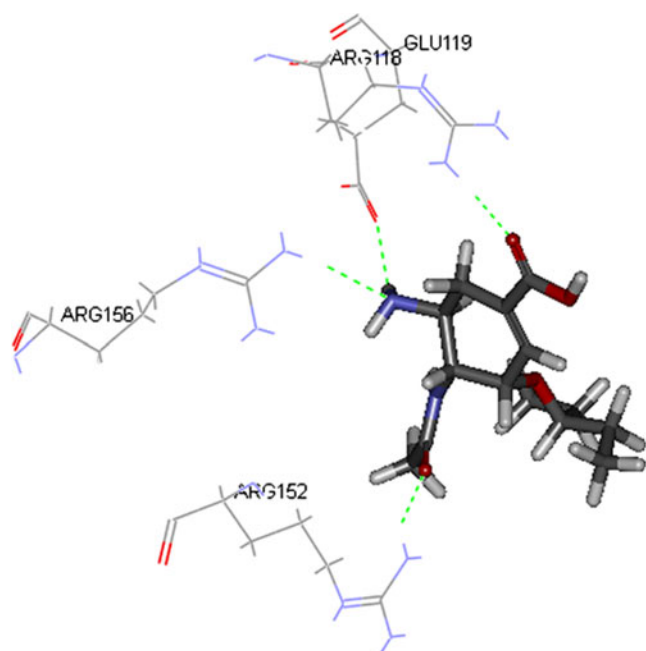


Fig. 9 Hydrogen bonds formed between oseltamivir and the active site of N1. Hydrogen bonds are shown by green dash line

were identified to be important amino acids in the pi-pi interaction. Furthermore, Arg293 of N1 also formed pi-pi interaction with ZINC02098378, which exhibited more total interaction energy than those with zanamivir and oseltamivir.

The structure differences of the two compounds from zanamivir, oseltamivir

The two novel compounds, ZINC02128091 and ZINC02098378, are composed with different chemical groups. ZINC02128091

Table 3 Hydrogen bond interaction parameters for each compound and N1 residue

Compound	Donors atom	Receptor atom	Distances(Å)
ZINC02128091	Arg293:HH22	ZINC02128091:O4	1.83
	Arg293:HH22	ZINC02128091:O20	2.43
	Arg368:HN	ZINC02128091:O29	2.19
	Arg368:HH22	ZINC02128091:O4	2.12
ZINC02098378	Arg293:HH22	ZINC02098378:O11	2.01
Zanamivir	Arg152:HH11	Zanamivir:O19	1.96
	Arg293:HH11	Zanamivir:O8	2.35
	Arg293:HH21	Zanamivir:O8	1.56
	Zanamivir:H36	Asp151:OD2	1.33
Oseltamivir	Arg118:HH11	Oseltamivir:O8	1.79
	Arg152:HH11	Oseltamivir:O14	1.97
	Arg156:HH22	Oseltamivir:N10	2.49
	Oseltamivir:H29	Glu119:OE1	2.34

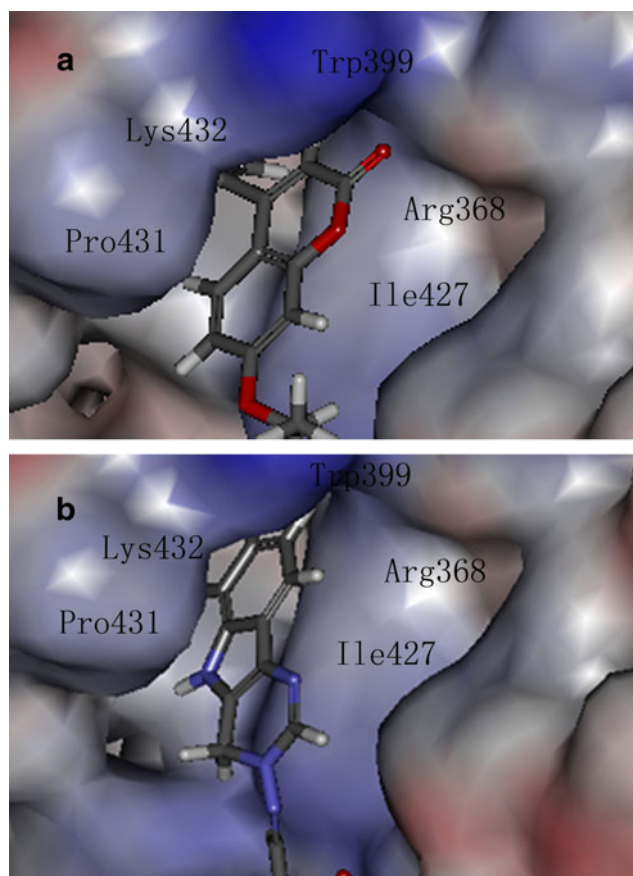


Fig. 10 Magnifying graphics of hydrophobic cave in Fig. 5, formed by Arg368, Trp399, Ile427, Pro431, Lys432 of N1, to bring a strong conjugation effect with compound (a) ZINC02128091, (b) ZINC02098378

is composed by coumarin modified α -hydroxy propionic acid moiety and indole-alanine derivative moiety (Fig. 4a). The indole-alanine derivative moiety of ZINC02128091 bound to the active pocket of N1 and coumarin modified α -hydroxy propionic acid moiety of this compound formed pi-pi interaction with Arg368 and Lys432 of N1 (Fig. 6). ZINC02098378 is a coumarin derivative with pyrimido-indole moiety (Fig. 4b). Different from ZINC02128091, coumarin derivative moiety of ZINC02098378 bound to the active pocket of N1 and formed pi-pi interaction with Arg293 of N1. Meanwhile,

Table 4 Pi-pi interaction parameters for each compound and N1 residue

Compound	End1	End2	Distances(Å)
ZINC02128091	ZINC02128091	Arg368:NE	4.12
	ZINC02128091	Arg368:NE	4.19
	ZINC02128091	Lys432:NZ	5.14
	ZINC02128091	Lys432:NZ	6.99
ZINC02098378	ZINC02098378	Arg293:NE	6.38
	ZINC02098378	Arg368:NE	4.18
	ZINC02098378	Arg368:NE	4.62

pyrimido-indole moiety formed pi-pi interaction with Arg368 of N1 (Fig. 7). In contrast to the two new compounds, the antiviral drug, zanamivir, is a carboxylic acid with acetamido, guanidino, pyran groups, while oseltamivir is an ene carboxylic acid with acetamido, pentan groups (Fig. 4c, d). These drugs bind to the active pocket of N1 and are structurally different from the two new compounds. In addition, ZINC02128091 and ZINC02098378 have more polycyclic groups, the number of skeleton carbons in the two positive antiviral drugs are only half of that in the new compounds and the molecular weights of these two new compounds are about 1.5 times greater than those of zanamivir and oseltamivir. Both of the two new compounds possess a phenyl-coumarin or pyrimido-indole group that could form pi-pi interaction with Arg293, Arg368 Lys432 of N1, which we called the hydrophobic head group in this paper, was absent in zanamivir and oseltamivir.

Worthy of note is that the compounds were virtually screened, and chemical synthesis experiment should be carried out if one wants a further study. In addition, the compounds were screened from NPD in the ZINC database, which predicted by ZINC as possible growth hormone secretion inhibitors. Therefore, the related biological experiments should also be tested besides the neuraminidase inhibition experiment.

Conclusions

In this study, the 3D structure of N1 was built by using homology modeling based on the known crystal structure of H5N1 avian influenza N1 (PDB ID: 3KCZ). By means of virtual screening technique, two novel compounds which effectively inhibited N1 have been found. Comparison with two effective drugs for N1, oseltamivir and zanamivir, the novel compounds screened exhibited very different structure characteristic. Then, the molecular docking method was used to verify the reliability of virtual screening and investigate the binding mechanism. Our docking results showed that the two novel compounds not only bound in the active pocket, but also formed pi-pi interaction with Arg293, Arg368 Lys432 of N1, which brings a strong conjugation effect. Consequently, the 3D structures of N1 bound with these two identified compounds revealed novel insights in the mode of inhibitory action and may provide basis for the design of new anti-influenza virus drugs.

Acknowledgments This work was supported by Chinese Ministry of Science and Technology (grant No. 2009IM031500), Chinese Ministry of Education (grant No. NCET-08-0244), National Natural Science Foundation of China (Grant No. 31100574), and the National Science Foundation of China (grant No. 31070638). We thank Dr. Oleg Trott for his kindness in offering us the AutoDock Vina program as a freeware.

References

1. Wang YT, Chan CH, Su ZY, Chen CL (2010) Homology modeling, docking, and molecular dynamics reveal HR1039 as a potent inhibitor of 2009 A(H1N1) influenza neuraminidase. *Biophys Chem* 147:74–80
2. Mercader AG, Pomilio AB (2010) QSAR study of flavonoids and flavonoids as influenza H1N1 virus neuraminidase inhibitors. *Eur J Med Chem* 45:1724–1730
3. WHO Memorandum Bulletin (1980) World-Health-Organization
4. Wiley DC, Skehel JJ (1987) The structure and function of the hemagglutinin membrane glycoprotein of influenza virus. *Annu Rev Biochem* 56:365–394
5. Murti KG, Webster RG (1986) Distribution of hemagglutinin and neuraminidase on influenza virions as revealed by immunoelectron microscopy. *Virology* 149:36–43
6. Liu AL, Wang HD, Lee SM, Wang YT, Du GH (2008) Structure–activity relationship of flavonoids as influenza virus neuraminidase inhibitors and their in vitro anti-viral activities. *Bioorg Med Chem* 16:7141–7147
7. McKimm-Breschkin JL (2000) Resistance of influenza viruses to neuraminidase inhibitors—a review. *Antiviral Res* 47:1–17
8. Du QS, Wang SQ, Chou KC (2007) Study of drug resistance of chicken influenza A virus (H5N1) from homology-modeled 3D structures of neuraminidases. *Biochem Biophys Res Commun* 354:634–640
9. Khan AU, Shakil S, Lal SK (2009) Efficacy of neuraminidase (NA) inhibitors against H1N1 strains of different geographical regions: an in silico approach. *Indian J Microbiol* 49:370–376
10. Yen HL, Ilyushina NA, Salomon R, Hoffmann E, Webster RG, Govorkova EA (2007) Neuraminidase inhibitor-resistant recombinant A/Vietnam/1203/04 (H5N1) influenza viruses retain their replication efficiency and pathogenicity in vitro and in vivo. *J Virol* 81:12418–12426
11. Kiso M, Mitamura K, Sakai-Tagawa Y, Shiraishi K, Kawakami C, Kimura K, Hayden FG, Sugaya N, Kawaoka Y (2004) Resistant influenza A viruses in children treated with oseltamivir: descriptive study. *Lancet* 364:759–765
12. Ison MG, Gubareva LV, Atmar RL, Treanor J, Hayden FG (2006) Recovery of drug-resistant influenza virus from immunocompromised patients: a case series. *J Infect Dis* 193:760–764
13. Li Y, Leung KT, Yao F, Ooi LS, Ooi VE (2006) Antiviral flavans from the leaves of pithecellobium clypearia. *J Nat Prod* 69:833–835
14. Miki K, Nagai T, Suzuki K, Tsujimura R, Koyama K, Kinoshita K, Furuhashi K, Yamada H, Takahashi K (2007) Anti-influenza virus activity of biflavonoids. *Bioorg Med Chem Lett* 17:772–775
15. Ginsburg H, Deharo E (2011) A call for using natural compounds in the development of new antimalarial treatments - an introduction. *Malar J* 10:S1
16. BioEdit (2011) BioEdit version 5.0.6. Caredata.com, Inc
17. Collins PJ, Haire LF, Lin YP, Liu J, Russell RJ, Walker PA, Skehel JJ, Martin SR, Hay AJ, Gamblin SJ (2008) Crystal structures of oseltamivir-resistant influenza virus neuraminidase mutants. *Nature* 453:1258–1261
18. Saisubramanian N, Edwinoliver NG, Nandakumar N, Kamini NR, Puvanakrishnan R (2006) Efficacy of lipase from *Aspergillus niger* as an additive in detergent formulations: a statistical approach. *J Ind Microbiol Biotechnol* 33:669–676
19. Arnold K, Bordoli L, Kopp J, Schwede T (2006) The SWISS-MODEL Workspace: A web-based environment for protein structure homology modeling. *Bioinformatics* 22:195–201
20. Schwede T, Kopp J, Guex N, Peitsch MC (2003) SWISS-MODEL: an automated protein homology-modeling server. *Nucleic Acids Res* 31:3381–3385

21. Guex N, Peitsch MC (1997) SWISS-MODEL and the Swiss-PdbViewer: an environment for comparative protein modeling. *Electrophoresis* 18:2714–2723
22. Nayeem A, Sitkoff D, Krystek S Jr (2006) A comparative study of available software for high-accuracy homology modeling: from sequence alignments to structural models. *Protein Sci* 15:808–824
23. Profile-3D User Guide (1999) Accelrys Inc, San Diego
24. Laskowski RA, MacArthur MW, Moss DS, Thornton JM (1993) PROCHECK: a program to check the stereochemical quality of protein structures. *J Appl Crystallogr* 26:283–291
25. Trott O, Olson A (2010) AutoDock Vina: improving the speed and accuracy of docking with a new scoring function, efficient optimization, and multithreading. *J Comput Chem* 31:455–461
26. Huey R, Morris GM, Olson AJ, Goodsell DS (2007) A semiempirical free energy force field with charge-based desolvation. *J Comput Chem* 28:1145–1152
27. Natural Products Database (NPD) (2011) http://wiki.compbio.ucsf.edu/wiki/index.php/Natural_products_database
28. Irwin JJ (2008) Using ZINC to acquire a virtual screening library. *Curr Protoc Bioinf* 22:14.6.1–14.6.23
29. Irwin JJ, Shoichet BK (2005) ZINC—a free database of commercially available compounds for virtual screening. *J Chem Inf Model* 45:177–182
30. Open Babel toolbox (2011) <http://openbabel.sourceforge.net/>
31. Raccoon (2011) <http://autodock.scripps.edu/resources/raccoon/>
32. Morris GM, Goodsell DS, Halliday RS, Huey R, Hart WE (1999) Automated docking using a Lamarckian genetic algorithm and an empirical binding free energy function. *J Comput Chem* 19:1639–1662
33. Affinity User Guide (1999) Accelrys Inc, San Diego
34. Insight II (2000) version 2000, Accelrys Inc, San Diego
35. Yu K, Luo C, Qin G, Xu Z, Li N, Liu H, Shen X, Ma J, Wang Q, Yang C, Zhu W, Jiang H (2009) Why are oseltamivir and zanamivir effective against the newly emerged influenza A virus (A/H1N1)? *Cell Res* 19:1221–1224
36. Kitchen D, Decornez H, Furr J, Bajorath J (2004) Docking and scoring in virtual screening for drug discovery: methods and applications. *Nat Rev Drug Discov* 3(11):935–949
37. Huanxiang L, Xiaojun Y, Chengqi W, Jian H (H1N1) In silico identification of the potential drug resistance sites over 2009 influenza A virus neuraminidase. *Mol Pharm* 7:894–904
38. Russell RJ, Haire LF, Stevens DJ, Collins PJ, Lin YP, Blackburn GM, Hay AJ, Gamblin SJ, Skehel JJ (2006) The structure of H5N1 avian influenza neuraminidase suggests new opportunities for drug design. *Nature* 443:45–49
39. Govorkova EA, Leneva IA, Goloubeva OG, Bush K, Webster RG (2001) Comparison of efficacies of RWJ-270201, zanamivir, and oseltamivir against H5N1, H9N2, and other avian influenza viruses. *Antimicrob Agents Chemother* 45:2723–2732
40. Bantia S, Parker CD, Ananth SL, Horn LL, Andries K, Chand P, Kotian PL, Dehghani A, El-Kattan Y, Lin T, Hutchison TL, Montgomery JA, Kellog DL, Babu YS (2001) Comparison of the anti-influenza virus activity of RWJ-270201 with those of oseltamivir and zanamivir. *Antimicrob Agents Chemother* 45:1162–1167
41. Boivin G, Goyette N (2002) Susceptibility of recent Canadian influenza A and B virus isolates to different neuraminidase inhibitors. *AntiViral Res* 54:143–147
42. Steiner T, Koellner G (2001) Hydrogen bonds with π -acceptors in proteins: frequencies and role in stabilizing local 3D structures. *J Mol Biol* 305:535–557
43. Weiss MS, Brandl M, Sühnel J, Pal D, Hilgenfeld R (2001) More hydrogen bonds for the (structural) biologist. *Trends Biochem Sci* 26:521–523
44. Hunter CA, Singh J, Thornton JM (1991) Pi-pi interactions: the geometry and energetic of phenylalanine-phenylalanine interactions in proteins. *J Mol Biol* 218:837–846